Computers and Concrete, *Vol. 14, No. 5 (2014) 577-597*
DOI: http://dx.doi.org/10.12989/cac.2014.14.5.577

Predictive models of hardened mechanical properties of waste LCD glass concrete

Chien-Chih Wang[1], Her-Yung Wang[*2] and Chi Huang[2]

[1]*Department of Civil Engineering and Geomatics, Cheng Shiu University, Kaohsiung, 833, Taiwan, R.O.C.*
[2]*Department of Civil Engineering, National Kaohsiung University of Applied Sciences, Kaohsiung, 807, Taiwan, R.O.C.*

(*Received June 9, 2014, Revised September 17, 2014, Accepted September 23, 2014*)

Abstract. This paper aims to develop a prediction model for the hardened properties of waste LCD glass that is used in concrete by analyzing a series of laboratory test results, which were obtained in our previous study. We also summarized the testing results of the hardened properties of a variety of waste LCD glass concretes and discussed the effect of factors such as the water-binder ratio (w/b), waste glass content (G) and age (t) on the concrete compressive strength, flexural strength and ultrasonic pulse velocity. This study also applied a hyperbolic function, an exponential function and a power function in a non-linear regression analysis of multiple variables and established the prediction model that could consider the effect of the water-binder ratio (w/b), waste glass content (G) and age (t) on the concrete compressive strength, flexural strength and ultrasonic pulse velocity.
Compared with the testing results, the statistical analysis shows that the coefficient of determination R^2 and the mean absolute percentage error (MAPE) were 0.93–0.96 and 5.4–8.4% for the compressive strength, 0.83–0.89 and 8.9–12.2% for the flexural strength and 0.87–0.89 and 1.8–2.2% for the ultrasonic pulse velocity, respectively. The proposed models are highly accurate in predicting the compressive strength, flexural strength and ultrasonic pulse velocity of waste LCD glass concrete. However, with other ranges of mixture parameters, the predicted models must be further studied.

Keywords: concrete; liquid crystal glasses; durability; mechanical properties; prediction model

1. Introduction

Since it was listed as the first-stage development priority of the "Two Trillion Core Industries Program", Taiwan's flat-panel display industry has flourished. Taiwan's output accounted for 38% of the global large-size LCD panel production in 2011, and it has become one of the largest producers of LCD panels, second only to Korea. With the substantial increase in production, large amounts of waste are derived from the manufacturing process (Gao *et al*. 2008).

The main chemical constituents of waste LCD glass are SiO_2, Na_2O and a small amount of indium-tin-oxide conducting film. The conducting film is coated on the LCD to reduce the

∗Corresponding author, Professor, E-mail: wangho@cc.kuas.edu.tw
[1]Associated Professor., E-mail: ccw@csu.edu.tw
[2]M.A. Candidate., E-mail: pupu522@hotmail.com

http://www.techno-press.org/?journal=cac&subpage=8 ISSN: 1598-8198 (Print), 1598-818X (Online)

resistance of the substrate surface, which enhances light transmittance and conductivity. Therefore, direct landfill, incineration and composting treatments are inappropriate for waste LCD glass (Lin, 2007). The glass contains a large amount of silicon and calcium and is classified as a Portland material. Its physical properties such as the unit weight, compressive strength, elasticity modulus, thermal expansion coefficient and heat transfer coefficient are notably close to concrete. Therefore, adding the crushed waste glass to concrete as a fine aggregate can reduce the concrete air content and unit weight, more efficiently pack the concrete pores, and provide better durability, surface resistance, resistance to acid, salt and alkali, chlorine iontophoresis, and better performance of the concrete ultrasonic pulse velocity (Topcu and Canbaz 2004; Wang *et al*. 2007; Huang 2009). Waste glass recycling can reduce the material cost, the effect on the environment and CO_2 emission, which are the preferred outcomes for sustainable environmental protection.

Although many studies have discussed concrete that is made with waste glass, most studies focus on the fresh and hardened properties test and seldom discuss the prediction model and regression analysis of the compressive strength, flexural strength and ultrasonic pulse velocity of the concrete. Therefore, based on the results of our previous studies on the mixture ratios of concrete with waste LCD glass (Huang 2009), this study aims to determine the relationships among the compressive strength, flexural strength, ultrasonic pulse velocity and the influencing factors such as the waste glass content, water-binder ratio and age. This study is expected to establish a waste glass concrete database and hardened properties prediction model, which will serve as references for mixing ratio research in the future.

2. Characteristics of glass and waste LCD glass concrete

Topcu and Canbaz (2004) used waste glass with a unit weight of 1493 kg/m^3~2400 kg/m^3 and a particle diameter of approximately 4-16 mm to replace coarse aggregate. The slump, air content and unit weight of the concrete decreased when the proportion of additional waste glass increased, but the slump flow, which is related to the workability, increased. In addition, the mechanical properties of concrete, such as the compressive strength, flexural strength, splitting tensile strength and dynamic modulus of elasticity decreased when the waste glass content increased. The concrete expansion slowed down when the addition of waste glass content increased. In addition, the results of Ismail and Hashmi (2009), who used recycled glass to partially replace the fine aggregate (maximum particle diameter of 20 mm and bulk density of 1545 kg/m^3), and Terro (2006), who used recycled crushed glass with different particle diameters as an aggregate, were observed to follow the same trend with those of Topcu and Canbaz.

Kou and Poon (2009) used recycled-glass sand with a particle diameter less than 5 mm, a specific gravity of 2.45 and a fineness modulus of 4.25 to study self-consolidating concrete (SCC). The findings indicated that the unit weight and air content decreased when the level of added waste glass increased. However, the decrease in amplitude was small, and the variance in slump flow was slightly influenced by the waste glass content. In addition, the expansion slowly increased when the level of added waste glass increased. The trends of the slump flow and the ASR test result (Kou and Poon 2009) were slightly different from the results of Topcu and Canbaz (2004). Regarding the mechanical properties, the compressive strength, splitting tensile strength and static elasticity modulus decreased when the waste glass content increased. Wang *et al*. (2011) found that the slump flow increased with the replacement of glass additive as an aggregate, but the

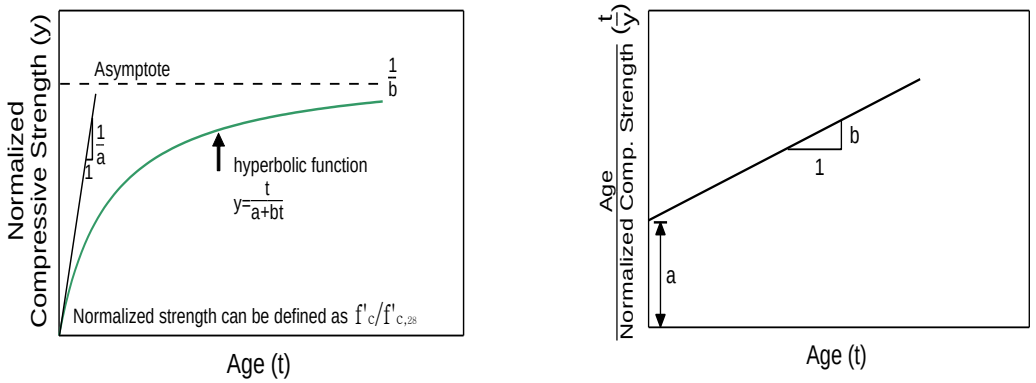

(a) Hyperbolic normalized compressive strength vs. curing age curve

(b) Transformed normalized compressive strength vs. curing age curve

Fig. 1 The characteristics of hyperbolic model

compressive strength and flexural strength decreased when the level of added glass increased. The compressive strength of waste LCD glass concrete also decreased when the replacement with waste glass increased (Park *et al*. 2004; Wang and Chen 2008; Wang 2009; Lin *et al*. 2012). However, according to the findings on using waste glass powder to replace concrete in case of high temperature, when the temperature increases, the compressive strength increases with the increase of the content. This trend differed from the observed mechanical properties of general recycled glass and waste LCD glass concrete (Ciou 2009). Furthermore, Tang (2014) also used a combination of waste TFT-LCD glass powder and reservoir sediments as lightweight aggregates. In summary, the waste LCD glass has been popularly employed in concrete production. Regarding the ultrasonic pulse velocity, because the glass sand has a smaller particle size than the normal-weight sand, it can fill the gap of the normal-weight sand and reduces the internal pores of the concrete. When the content of waste glass sand increases, the ultrasonic pulse velocity also increases. However, when the water-binder ratio and the mixing water content increase, the concrete is prone to pores, which affects the velocity passes. Therefore, the ultrasonic pulse velocity tends to decline with increasing water-binder ratio (Huang 2009).

As previously mentioned, the compressive strength and flexural strength of the concrete with the replacement of recycled glass, waste glass or waste LCD glass as aggregates primarily decrease when the addition level increases. However, the ultrasonic pulse velocity increases accordingly. In addition, the compressive strength, flexural strength and ultrasonic pulse velocity of the concrete with waste glass are similar to the behavioral characteristics of general concrete; the compressive strength, flexural strength and ultrasonic pulse velocity increase with the curing time. However, after a certain age, the increase in compressive strength, flexural strength and ultrasonic pulse velocity becomes smooth. Similarly, the compressive strength, flexural strength and ultrasonic pulse velocity decrease when the water-binder ratio increases.

3. Experimental materials and mixtures

This study integrated a series of test results with different mixture ratios of self-compacting

waste LCD glass concrete to discuss the relationships among multiple influencing factors of compressive strength, flexural strength and ultrasonic pulse velocity, waste glass content, water-binder ratio and age to establish predictive analysis models to evaluate the compressive strength, flexural strength and ultrasonic pulse velocity. The material properties and mixture content ratios are briefly described below (Huang 2009; Wang and Huang 2010a; Wang and Huang 2010b).

The cement, fly ash, and slag that were used in this study were local materials that complied with the specifications in CNS61, CNS3036, and CNS12549, respectively. Particulate waste glass sand, which could pass through a No. 8 sieve, was provided by Chi Mei Optoelectronics. Type 1000 superplasticizer, which complied with the ASTM C494 type G admixture, was used. The water-to-binder ratios were 0.28, 0.32, and 0.36, and 4 types of glass sand were added at volume replacement ratios of 0%, 10%, 20%, and 30%. Fly ash, water-quenched slag and superplasticizer were added and blended using a simple SCC mixing design method to explore the mixing, hardening and durability properties. The compressive strength, flexural strength, ultrasonic pulse velocity, and several other parameters were measured. The physical properties of the aggregate and glass sand, the SCGC mixture proportions, and the particle-size distribution curves of the aggregate and glass sand can be referred in our previous study (Wang and Huang 2010a; Wang and Huang 2010b).

4. Studying and planning the prediction model for the compressive strength, flexural strength and ultrasonic pulse velocity

Vahid, K.A. and Mohammad, T. (2010) predicted the 28-day compressive strength of concrete using artificial neural networks and found that the compressive strength of concrete increased with age, but the trend became smooth over time. The relationship was an approximately horizontal curve after a certain age. The results of other studies on the compressive strength of concrete revealed the same trend (Lin *et al*. 2012; Hwang *et al*. 1999; Lin *et al*. 2009; Mousavi *et al*. 2012; Murat *et al*. 2007). The relationship curve of the compressive strength and age is notably close to the non-linear stress-strain relationship of soil, which is assessed by many scholars using the hyperbolic model (Konder 1963; Duncan and Chang 1970; Sridharan and Rao 1972; Boscardin *et al*. 1990; Stark *et al*. 1994; Wang 2001; Al-Shamrani 2005). Therefore, as long as variables are appropriately changed, the hyperbolic model can be applied to predictive analysis to determine the trends in the compressive strength of concrete, and the results as shown in Figs. 1(a) and 1(b). Here, 1/a represents the initial slope of the strength curve, which indicates the growth of the initial strength. Additionally, 1/b represents the asymptotes of the strength curve, and it is also the highest value of the compressive strength.

In addition, with respect to the influence of additives in concrete on the compressive strength, including the influence of the replacement with fly ash, furnace slag and waste glass for partial cement or sandy soil under identical conditions, the compressive strength of the concrete with any additive increased with age, and the increase in compressive strength became smooth over time. According to the findings on waste glass concrete, the compressive strength declines with increasing ratio of waste glass content (Topcu and Canbaz 2004; Terro 2006; Kou and Poon 2009; Wang 2011; Park *et al*. 2004; Wang and Chen 2008; Wang 2009; Lin *et al*. 2012). Furthermore, according to the flexural strength research results of various types of concretes, the flexural strength tends to increase with rising age and follows an identical trend with the concrete compressive strength. The ratio between the flexural strength and the compressive strength is in

the range of 10%~20% (Ahmed, 2013; Atis *et al*. 2009; Cheng *et al*. 2011; Barbuta *et al*. 2012; Dapena *et al*. 2011; Kumar *et al*. 2007). Therefore, we may infer the bending-strength prediction model by considering the ratio of the flexural strength and the compressive strength.

Before the damage, the ultrasonic pulse velocity and compressive strength of the concrete are in a linearly increasing relationship. Most studies on the ultrasonic pulse velocity of waste glass concrete suggest that the ultrasonic pulse velocity tends to increase with increasing content of waste glass (Huang 2009; Wang and Chen 2008; Wang 2009; Wang and Huang 2010b). Shah *et al*. (2012) applied the neural network to predict the residual strength of the damaged concrete, which found that the residual strength could be reasonably predicted and analyzed using the non-linear ultrasonic pulse velocity. In addition, according to the findings on waste LCD glass concrete by Wang (2009), the ultrasonic pulse velocity has the same tendency with the compression strength and the flexural strength and increases with rising age. However, it tends to become smooth after a certain period of time.

Therefore, based on the hyperbolic model, we considered a number of variables including the water-binder ratio w/b, age t and waste glass substitution percentage G to deduce the waste LCD glass concrete compressive-strength prediction model. We also developed the flexural-strength prediction model in terms of the flexural strength and compressive strength ratio. Finally, we explored the non-linear relationship between the ultrasonic pulse velocity and the age using a power function.

4.1 Development of the compressive-strength prediction model

The compressive strength of waste glass concrete decreases when the level of added waste glass increases (Topcu and Canbaz 2004; Terro 2006; Kou and Poon 2009; Wang 2011; Park *et al*. 2004; Wang and Chen 2008; Wang 2009; Lin *et al*. 2012). Therefore, the model in this study assumes that the compressive strength of the waste glass concrete decreases when the waste glass content increases using an identical mixture ratio.

Fig. 2 shows the test result of a normalized ratio of the compressive strength at different curing ages and on Day 28 with a water-binder ratio w/b of 0.28 and a waste glass replacement ratio G of 0~30%. For an identical waste glass content G, the compressive strength f'_c increases with the age t, but the increase becomes smooth when the age further increases. Similar phenomena were observed in other tests with various water-binder ratios. Therefore, the relation between the compressive strength and the age is simulated using the hyperbolic model, as shown in Eq. (1), where parameters a_c and b_c (shown in Table 1) are the coefficients of a hyperbolic function, and t is the age. Under the identical conditions, parameter a_c increases with the waste glass content based on the assumption that the compressive strength decreases when the waste glass content increases. Thus, a linear increasing function between a_c and G was used and shows that a_c is parallel related to the change in waste glass content, as shown in Fig. 3(a). Therefore, in the model deduction, it is assumed that parameter a_c and waste glass content G are in a linearly increasing relationship that can be described as shown in Eq. (2). Parameters m and α are the linear-relationship intercept and slope, respectively. Furthermore, detailed discussion was focused on the relationship between parameters m and water-binder ratio w/b. Parameters m and w/b also exhibit a linear increasing relationship, as approximated in Eq. (3). Table 1 shows that parameter b_c did not affected various waste glass contents; therefore, no relationship is found as shown in Fig. 3(b), and the sensitivity of parameter b_c is expressed as shown in Eq. (4). Similarly, a linear decreasing relationship between the parameter n and the water-binder ratio w/b is shown in Eq. (5).

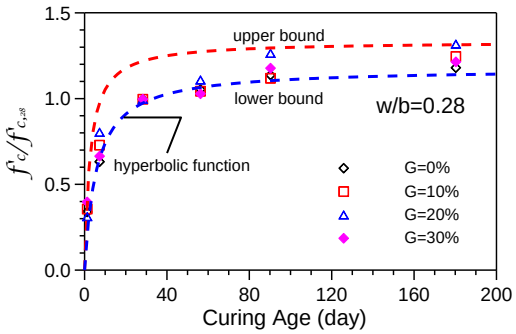

Fig. 2 Normalized compressive strength vs. curing time

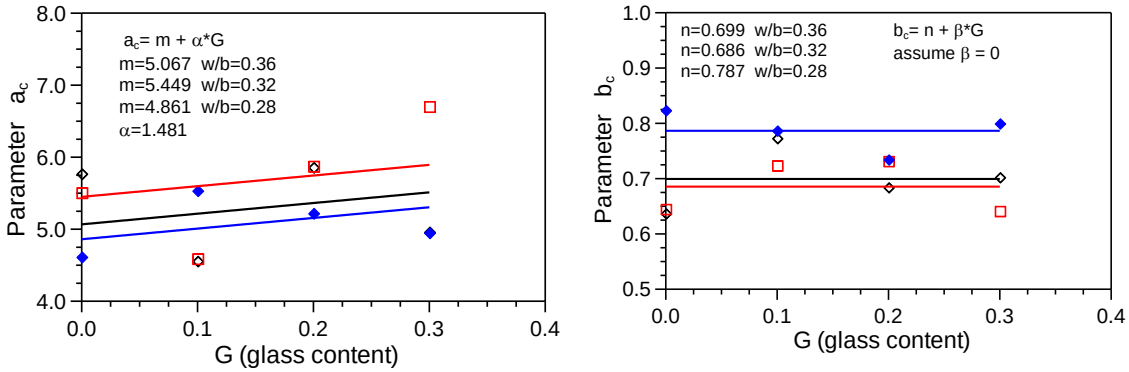

(a) Parameter a_c of hyperbolic function vs. glass content

(b) Parameter b_c of hyperbolic function vs. glass content

Fig. 3 The characteristics of parameters of compressive strength predicted model

Table 1 Values of parameter a_c, b_c, a_s and b_s for different mixtures.

w/b	G	a_c	b_c	a_s	b_s
0.28	0	4.616	0.824	3500	0.040
	0.1	5.538	0.787	3509	0.042
	0.2	5.224	0.735	3606	0.039
	0.3	4.952	0.800	3764	0.032
0.32	0	5.510	0.645	3420	0.043
	0.1	4.593	0.724	3422	0.046
	0.2	5.877	0.732	3523	0.042
	0.3	6.706	0.642	3456	0.050
0.36	0	5.773	0.637	3273	0.051
	0.1	4.560	0.773	3307	0.052
	0.2	5.862	0.685	3458	0.045
	0.3	4.964	0.703	3466	0.048

Table 2 The value of parameters of predicted model

Compressive strength model		Flexural strength model		Ultrasonic pulse velocity model	
parameters	value	parameters	value	parameters	value
a	1.48	b_t	-3.347	a_s	610
ß	0	m_t	0.212	$ß_s$	-0.0145
θ	-5.10	n_t	4.815×10^{-4}	m_{s1}	4258.7
m_1	4.30	—	-	m_{s2}	-2732.5
m_2	2.58	-	-	n_{s1}	0.0037
n_1	1.07	-	-	m_{s2}	0.1331
n_2	-1.09	-	-	-	-
x_1	124.2	-	-	-	-
x_2	-214.3	-	-	-	-

$$y=\frac{f'_c}{f'_{c,28}}=f(t)=\frac{t}{a_c+b_c} \tag{1}$$

$$a_c=f(G)=(m+\alpha\times G) \tag{2}$$

$$m=(m_1+m_2(w/b)) \tag{3}$$

$$b_c=f(G)=(n+\beta\times G) \tag{4}$$

$$n=(n_1+n_2(w/b)) \tag{5}$$

where a, ß, m and n are the parameters that are related to the waste glass content G, and m_1, m_2 and n_1, n_2 are the coefficients that are related to water-binder ratio (w/b). Eqs. (2)-(5) are combined, and Eq. (1) can be expressed as Eq. (6). The evaluation method for the compressive strength on Day 28 is derived and expressed as Eq. (7). When the prediction model for the compressive strength of concrete is used for the model regression analysis of the test results, the model parameters are α = 1.48, ß = 0, θ = -5.10, m_1=4.30, m_2 = 2.58, n_1 = 1.07, n_2 = -1.09, x_1 = 124.2, x_2 = -214.3 and tabulated in Table 2. More information of compressive strength prediction model can be referred in our previous study (Wang *et al*. 2014).

$$\frac{f'_c}{f'_{c,28}}=\frac{t}{[(m_1+m_2(w/b))+\alpha\times G]+[(n_1+n_2(w/b))+\beta\times G]\times t} \tag{6}$$

$$f'_{c,28}=[x_1+x_2(w/b)]+\theta\times G \tag{7}$$

4.2 Development of the flexural-strength prediction model

The flexural strength and age relationship curve is similar to the development trend of the concrete compressive strength. Moreover, the flexural strength and compressive strength ratio is in a certain range (Ahmed 2013; Atis *et al*. 2009; Cheng *et al*. 2011; Barbuta *et al*. 2012; Dapena *et al*. 2011; Kumar *et al*. 2007). Therefore, we can deduce the flexural strength model by bending and compressive the strength ratio relationship. According to the waste LCD glass concrete testing results, when the water-binder ratio is 0.36, the ratio of the flexural strength and the compressive strength f'_t/f'_c and the waste glass content do not significantly change as shown in Fig. 4. The other water-binder ratios have the same testing results. Therefore, in the model deduction, we

assumed that the f'_t/f'_c ratio and the waste glass content were not related. As shown in Fig. 5(a), when the concrete was aged for 28 days, the f'_t/f'_c ratio significantly declined with increasing water-binder ratio, and the relationship can be simulated using an exponential function. The same trends can be observed in the event of other ages as shown in Fig. 5(b). Moreover, the f'_t/f'_c ratio and the water-binder ratio relationship curves are parallel curves for different ages and tend to gradually increase as shown in Figs. 5(a) and 5(b).

In the model deduction, we assumed that the waste glass concrete bending and compressive strength f'_t/f'_c ratio had a gradually decreasing relationship in the form of an exponential function when the water-binder ratio w/b increased for the same mixing ratio as shown in Eq. (8). The declining relationships of the non-linear regression are parallel curves for different ages; hence, parameter b_t is roughly a constant. Parameter a_t is the non-linear regression curve intercept. According to the analysis results, parameter a_t and the age are roughly in a linearly increasing relationship as shown in Fig. 6, and parameter a_t can be represented as shown in Eq. (9). By integrating Eqs. (8) and (9), we obtain the flexural strength prediction model as shown in Eq. (10). The compressive strength f'_c can be estimated using the aforementioned Eqs. (6) and (7). It is noteworthy that in the deduction of the flexural strength model, the f'_t/f'_c ratio is assumed to be free from the effect of the waste glass content and is only related to the water-binder ratio w/b. Therefore, although the effect of the waste glass content G on the flexural strength f'_t cannot be observed in Eq. (10), it is implied when the compressive strength f'_c value is estimated.

$$\frac{f'_t}{f'_c} = a_t \times \exp(b_t \times w/b) \tag{8}$$

$$a_t = (m_t + n_t \times t) \tag{9}$$

$$f'_t = (m_t + n_t \times t) \times \exp(b_t \times (w/b)) \times f'_c \tag{10}$$

where a_t and b_t are the parameters that are related to the water-binder ratio (w/b), and m_t and n_t are the coefficients that are related to age (t). When the prediction model for the flexural strength of concrete is used for the model regression analysis of the test results, the model parameters are b_t = -3.347, m_t = 0.212, n_t = 4.815×10^{-4} and tabulated in Table 2.

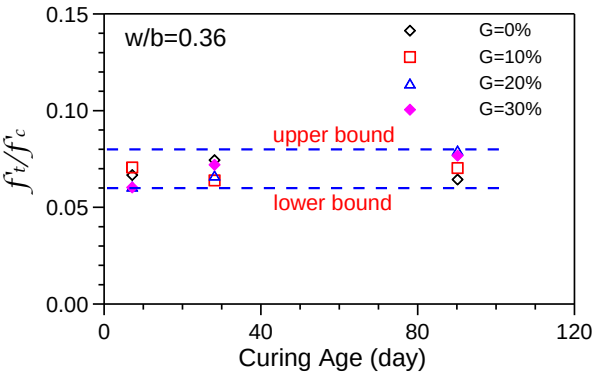

Fig. 4 Flexural strength and compressive strength ratio vs. curing time

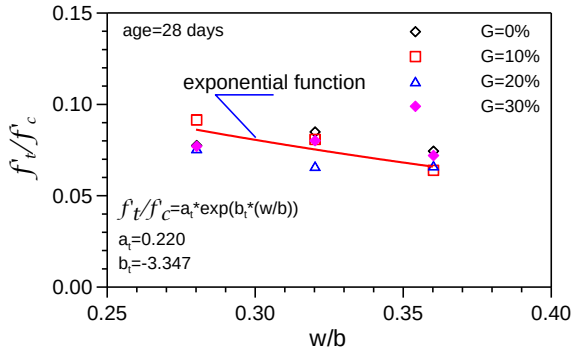

(a) Relationship of measured data and estimated values for curing age on Day 28

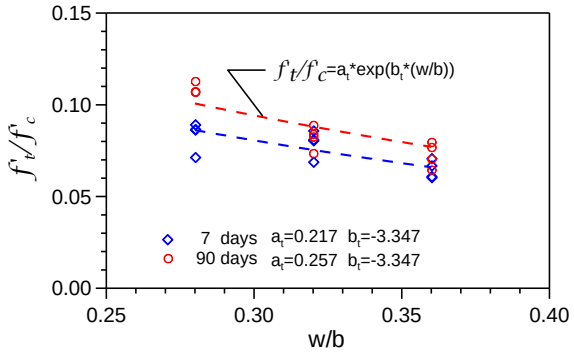

(b) Relationship of measured data and estimated values for curing age on Day 7 and 90

Fig. 5 Flexural strength and compressive strength ratio vs. water-binder ratio

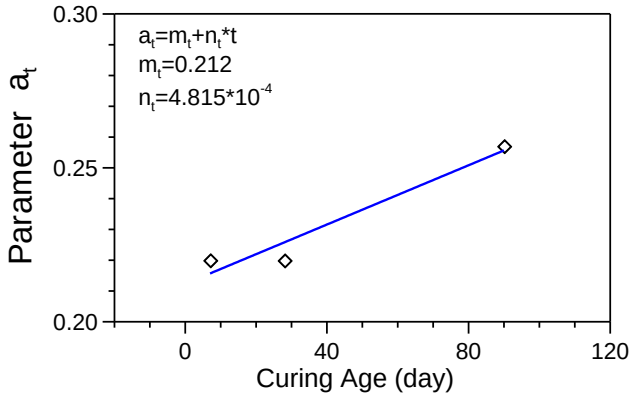

Fig. 6 Relationship of parameter a_t vs. curing age

4.3 Development of the ultrasonic-pulse-velocity prediction model

The ultrasonic pulse velocity tends to increase with increasing waste glass content and maintenance age. However, after a period of time, the increase of the ultrasonic pulse velocity tends to become smooth (Huang 2009; Wang and Chen 2008; Wang, 2009; Wang and Huang 2010a; Wang and Huang 2010b). In the model deduction, it is assumed that the ultrasonic pulse velocity of waste glass concrete tends to increase with increasing waste glass content for the same mixing ratio. In addition, at the initial maintenance stage after mixing the concrete, the concrete gradually becomes hardened from the flowing state of the initial setting to the solid stage of the final setting. Therefore, its mechanical properties significantly change. In other words, the specimen should be aged for one day to have the appropriate compressive strength; therefore, its ultrasonic pulse velocity is considerable. Hence, in the deduction of the ultrasonic-pulse-velocity prediction model, the sharp rise in the ultrasonic pulse velocity of the concrete after the initial setting and the gradually smoothing properties of the ultrasonic pulse velocity should be simulated. Fig. 7 illustrates the testing results of the concrete ultrasonic pulse velocity and age for different waste glass contents when the water-binder ratio is 0.28. For the same waste glass content G, the ultrasonic pulse velocity V_s increases with the age t, but the increase becomes smooth as the age

further increases. Therefore, the relation between the ultrasonic pulse velocity and the age is simulated using a power function, as shown in Eq. (11), where parameters a_s and b_s (shown in Table 1) are the coefficients of the power function, and t is the age.

Under identical age condition, the ultrasonic pulse velocity tends to increase with increasing amount of waste glass; similar phenomena were observed in other tests with various water-binder ratios. It is noteworthy that under identical conditions, parameter a_s increases with the waste glass content. Moreover, for different water-binder ratios, the trend tends to be a linear relationship of mutual parallel lines as shown in Fig. 8(a). Therefore, in the model deduction, if parameter a_s and the waste glass content G are in a linearly increasing relationship, it can be described as shown in Eq. (12). Parameters m_s and α_s are the linear-relationship intercept and slope, respectively.

Furthermore, the relationship between parameter m_s and the water-binder ratio w/b is linearly decreasing as shown in Fig. 8(b) and expressed as Eq. (13). Similarly, the relationship between parameters b_s and the waste glass contents is linearly decreasing as shown in Fig. 8(c) and

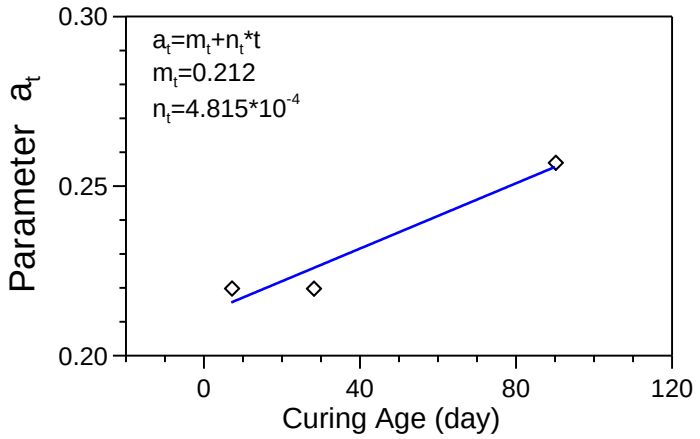

Fig. 6 Relationship of parameter a_t vs. curing age

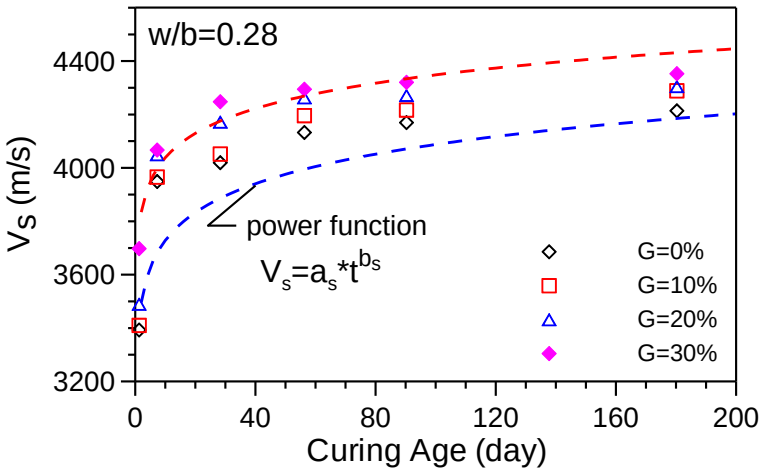

Fig. 7 Ultrasonic pulse velocity vs. curing age

expressed as Eq. (14). Parameters n_s and $ß_s$ are the linear-relationship intercept and slope, respectively. The relationship between parameter n_s and the water-binder ratio w/b is linearly increasing as shown in Fig. 8(d) and expressed as Eq. (15).

$$V_s = a_s \times t^{b_s} \tag{11}$$

$$a_s = m_s + \alpha_s \times G \tag{12}$$

$$m_s = m_{s1} + m_{s2} \times (w/b) \tag{13}$$

$$b_s = n_s + \beta_s \times G \tag{14}$$

$$n_s = n_{s1} + n_{s2} \times (w/b) \tag{15}$$

$$V_S = (m_{s1} + m_{s2} \times (w/b) + \alpha_s \times G) \times t^{(n_{s1}+n_{s2}\times(w/b)+\beta_s \times G)} \tag{16}$$

where a_s , $ß_s$, m_s and n_s are the parameters that are related to the waste glass content (G), and m_{s1}, m_{s2} and n_{s1}, n_{s2} are the coefficients of the water-binder ratio (w/b). Eqs. (11) to (15) are combined, and the ultrasonic-pulse-velocity prediction model is described as shown in Eq. (16). When the prediction model of the waste glass concrete ultrasonic pulse velocity is applied in the regression analysis of the testing results, the model parameters are a_s = 610, $ß_s$ = -0.0145, m_{s1} = 4258.7, m_{s2} = -2732.5, n_{s1} = 0.0037, n_{s2} = 0.1331 and tabulated in Table 2.

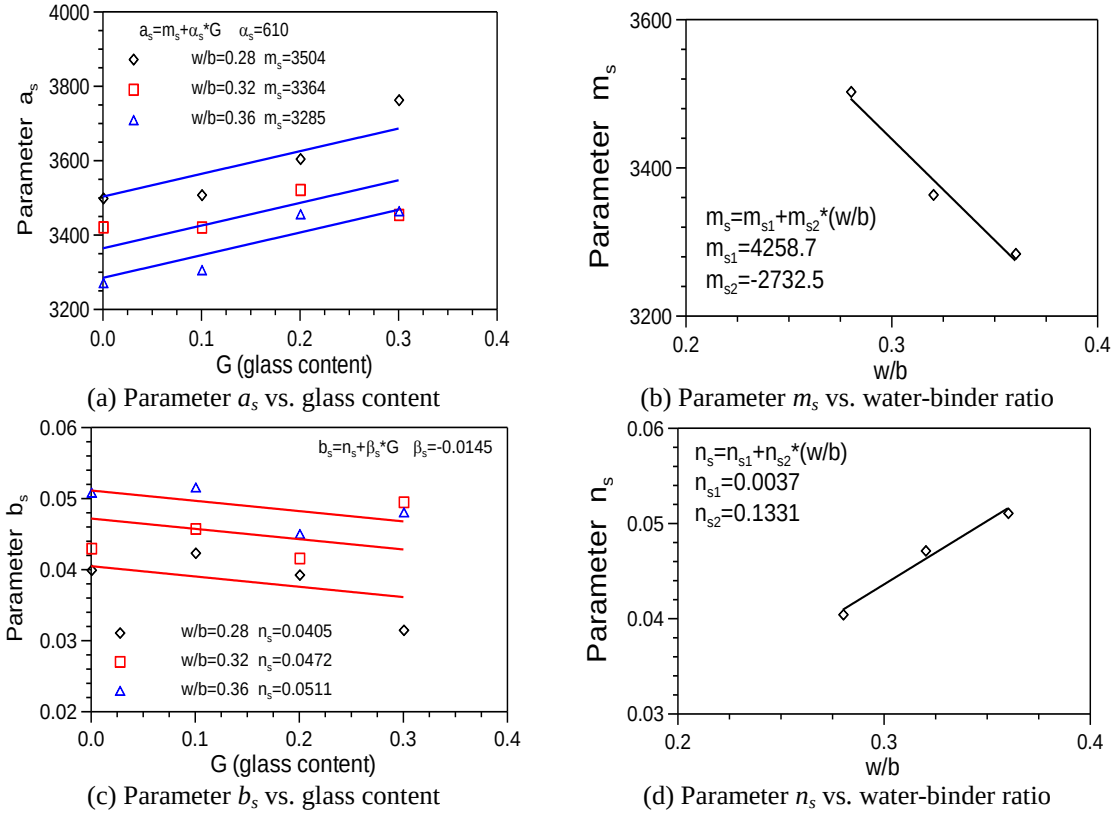

(a) Parameter a_s vs. glass content

(b) Parameter m_s vs. water-binder ratio

(c) Parameter b_s vs. glass content

(d) Parameter n_s vs. water-binder ratio

Fig. 8 The characteristics of parameters of ultrasonic pulse velocity predicted model

5. Comparison between the predictive analysis and the test result

The MAPE (mean absolute percentage error) of Eq. (17) can be used to determine the error between the model analysis result and the measured value (Lewis 1982). If the MAPE is less than 10%, the model has excellent predictive ability; if the MAPE is in the range of 10-20%, the model has good predictive ability; if the MAPE is more than 50%, the prediction results of the model are not accurate. Notably, Mousavi *et al*. (2012) studied high-performance concrete and found that when comparing the analytical result of a prediction model and the experimental value, if the coefficient of determination R^2 is greater than 0.8, there is an excellent correlation. Therefore, we adopted the MAPE and R^2 values to determine the accuracy of various types of prediction models.

$$MAPE = \frac{1}{k}\sum_{i=1}^{k}\left|\frac{y_i - \hat{y}_i}{y_i}\right| \tag{17}$$

where y_i = measured value, $\hat{y}_i$ = model analysis value, and k = number of analytic data.

5.1 Compressive strength

As shown in Figs. 9(a) and 10(b), the multivariate concrete compressive-strength prediction model, which considers the water-binder ratio w/b, age t and waste glass content G in the previous section, is used to compare with the test results for waste glass content G = 0 and G = 30%. As the analysis results suggest, the compressive-strength prediction model based on the hyperbolic model can accurately evaluate the compressive strength at different w/b, t and G conditions. In addition, Fig. 10 illustrates the prediction analysis values and the testing results of waste glass concrete compressive strength for different ages when the water-binder ratio is 0.36. As the analysis results suggest, the proposed compressive-strength prediction model can be used to reasonably estimate the compressive strength of concretes of different waste glass contents. The prediction analysis results of other water-binder ratios and waste glass contents suggest the same trends. The comparison of the predicted values of compressive strength using the model and the actual experimental values was shown in Table 3.

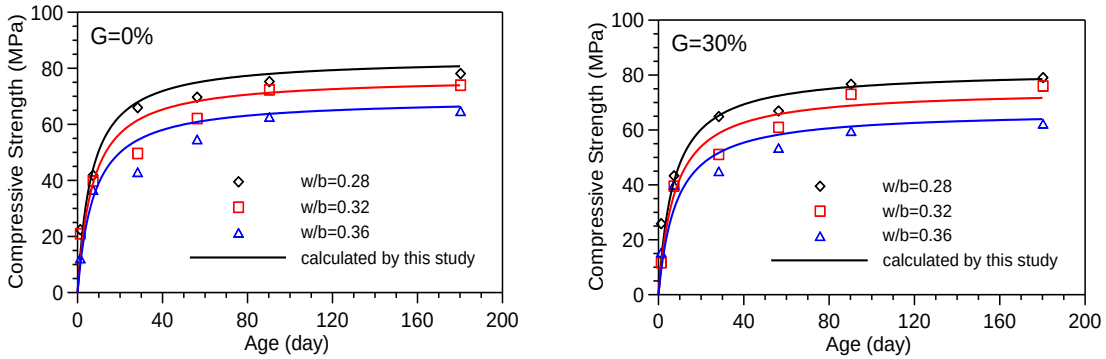

(a) Glass content is 0% (b) Glass content is 30%

Fig. 9 Comparison results of predicted model and test results for compressive strength

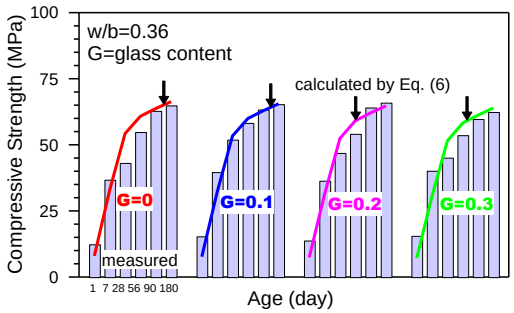

Fig. 10 Comparison results of predicted model and test results for compressive strength at w/b=0.36

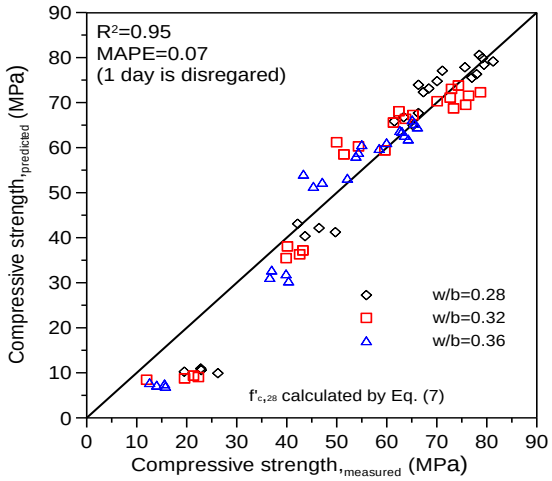

Fig. 11 Comparison of predicted and measured compressive strength

Table 3 Comparison of predicted and measured values of compressive strength

w/b	No.	Tested compressive strength (MPa)						Predicted compressive strength (MPa)					
	Age (day)	1	7	28	56	90	180	1	7	28	56	90	180
0.28	SC28G0	22.67	42.05	66.19	69.93	75.50	78.35	11.09	43.23	67.80	74.89	77.97	80.71
	SC28G10	22.75	46.32	63.26	66.20	70.97	79.01	10.72	42.28	66.89	74.07	77.20	79.99
	SC28G20	19.38	49.58	61.38	68.27	77.82	81.13	10.38	41.36	65.98	73.25	76.43	79.26
	SC28G30	26.11	43.52	65.12	67.17	76.89	79.30	10.05	40.47	65.09	72.44	75.66	78.54
0.32	SC32G0	21.21	40.00	49.84	62.30	72.55	74.19	9.50	38.19	61.33	68.21	71.23	73.93
	SC32G10	22.21	43.10	54.21	65.10	69.94	72.82	9.18	37.30	60.41	67.37	70.43	73.17
	SC32G20	19.44	42.44	59.48	63.61	75.65	78.60	8.88	36.44	59.51	66.53	69.63	72.41
	SC32G30	11.84	39.76	51.30	61.20	73.23	76.23	8.59	35.59	58.61	65.70	68.84	71.66
0.36	SC36G0	12.44	36.85	43.21	54.87	62.90	64.96	7.96	32.96	54.26	60.81	63.71	66.32
	SC36G10	15.43	39.73	51.99	58.34	63.40	65.41	7.68	32.13	53.35	59.94	62.88	65.53
	SC36G20	13.86	36.48	46.97	54.20	64.15	65.99	7.41	31.32	52.44	59.09	62.06	64.74
	SC36G30	15.61	40.24	45.20	53.69	59.82	62.48	7.16	30.53	51.55	58.23	61.23	63.94

Table 4 Comparison of predicted and measured values of flexural strength

w/b	No.	Tested flexural strength (MPa)			Predicted flexural strength (MPa)		
	Age (day)	7	28	90	7	28	90
0.28	SC28G0	3.80	5.15	8.10	3.65	6.00	7.81
	SC28G10	4.01	5.81	8.02	3.57	5.92	7.73
	SC28G20	3.55	4.68	8.36	3.50	5.84	7.65
	SC28G30	3.78	5.04	8.24	3.42	5.76	7.58
0.32	SC32G0	3.25	4.25	5.35	2.82	4.74	6.24
	SC32G10	3.71	4.40	5.89	2.76	4.67	6.17
	SC32G20	2.93	3.96	6.74	2.69	4.60	6.10
	SC32G30	3.21	4.13	6.06	2.63	4.54	6.03
0.36	SC36G0	2.47	3.23	4.07	2.13	3.67	4.88
	SC36G10	2.82	3.34	4.48	2.08	3.61	4.82
	SC36G20	2.23	3.14	5.12	2.02	3.55	4.76
	SC36G30	2.44	3.27	4.61	1.97	3.49	4.69

Table 5 Comparison of predicted and measured values of ultrasonic plus velocity

w/b	No.	Tested ultrasonic pulse velocity (m/s)						Predicted ultrasonic pulse velocity (m/s)					
	Age (day)	1	7	28	56	90	180	1	7	28	56	90	180
0.28	SC28G0	3396	3952	4023	4136	4173	4217	3494	3783	4004	4119	4200	4321
	SC28G10	3413	3969	4055	4199	4220	4292	3555	3839	4054	4167	4246	4364
	SC28G20	3493	4053	4175	4266	4275	4308	3616	3893	4104	4214	4291	4405
	SC28G30	3701	4070	4251	4298	4324	4356	3677	3948	4153	4260	4335	4446
0.32	SC32G0	3329	3849	4035	4062	4137	4190	3384	3703	3948	4077	4168	4303
	SC32G10	3329	3868	4063	4120	4195	4241	3445	3759	4000	4126	4215	4348
	SC32G20	3418	3968	4128	4181	4213	4279	3506	3815	4051	4175	4262	4392
	SC32G30	3303	4051	4162	4218	4282	4343	3567	3870	4102	4223	4308	4435
0.36	SC36G0	3175	3750	3962	4020	4103	4158	3275	3621	3889	4031	4131	4281
	SC36G10	3203	3791	4036	4082	4165	4196	3336	3678	3943	4082	4180	4328
	SC36G20	3341	3933	4122	4160	4212	4247	3397	3735	3995	4132	4229	4374
	SC36G30	3344	3969	4186	4217	4282	4317	3458	3791	4047	4182	4277	4419

Table 6 Values of R^2 and MAPE for predictive analysis and test result

	compressive strength		flexural strength		ultrasonic pulse velocity	
w/b	R^2	MAPE	R^2	MAPE	R^2	MAPE
0.28	0.96	0.054	0.89	0.089	0.88	0.018
0.32	0.93	0.074	0.83	0.117	0.87	0.021
0.36	0.95	0.084	0.85	0.122	0.89	0.022

To validate the accuracy of the prediction model analysis results, this study employs two indices: the MAPE and R^2 to determine the error between the model analysis result and the measured value. The coefficient of determination R^2 was obtained from the regression analysis using the model for the predicted compressive strength analysis value and the test result. When w/b is 0.28, R^2=0.96; when w/b is 0.32, R^2=0.95; when w/b is 0.32, R^2=0.93. The analytic result shows that when the water-binder ratios w/b are 0.28, 0.32 and 0.36 and the test result at the age of one day is disregarded, the MAPE values are 5.4%, 7.4% and 8.4%, respectively. The comparison of all water-binder ratio analysis values and testing results suggest that the coefficient of determination is R^2 = 0.95, which is greater than 0.8, and MAPE=7.0%, which is lower than 10% as shown in Fig. 11 and Table 6. Therefore, the compressive-strength prediction model that was reported in this paper has excellent prediction abilities

5.2 Flexural strength

As shown in Figs. 12(a) and 12(b), the flexural-strength prediction model (Eq. (10)) is applied in the flexural-strength analysis and the testing results for the waste glass content G = 0% and G=30% for different water-binder ratios. Fig. 13 illustrates the comparison of the prediction analysis and the testing results of the flexural strength for concretes of different waste glass contents and ages when the water-binder ratio is 0.36. As shown in Fig. 13, the flexural-strength prediction model based on an exponential function can accurately evaluate the flexural strength at different w/b, t and G values. The comparison between the predicted flexural-strength values using the model and the actual experimental values was shown in Table 4.

In addition, the coefficient of determination R^2 was obtained from the regression analysis using the model for the predicted flexural-strength analysis value and the test result: when w/b is 0.28, R^2 = 0.89; when w/b is 0.32, R^2 = 0.83; when w/b is 0.36, R^2 = 0.85. The analytical result shows that the MAPE value is 8.9%, 11.7% and 12.2% when the water-binder ratio w/b is 0.28, 0.32 and 0.36, respectively. The comparison of all water-binder ratio analysis values and testing results suggest that the coefficient of determination is R^2 = 0.90, which is greater than 0.8, and MAPE = 10.0%, as shown in Fig. 14 and Table 6. Therefore, the flexural-strength prediction model also has good prediction capabilities.

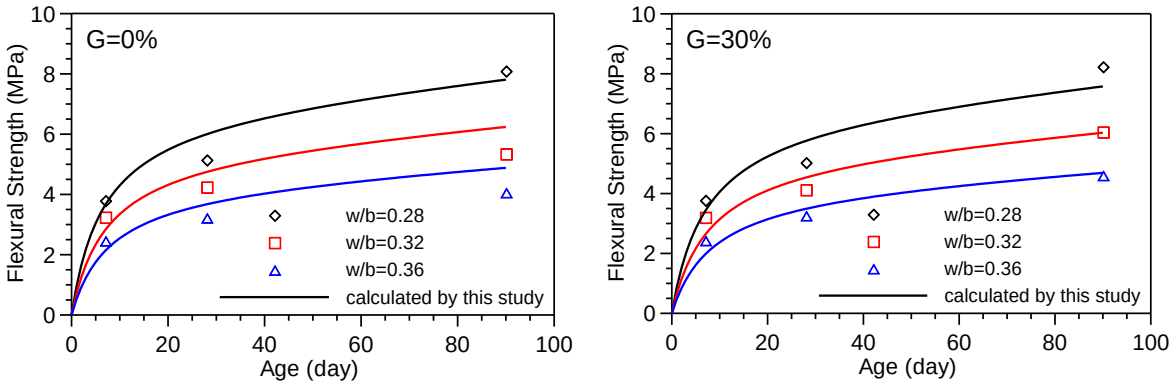

(a) Glass content is 0% (b) Glass content is 30%

Fig. 12 Comparison results of predicted model and test results for flexural strength

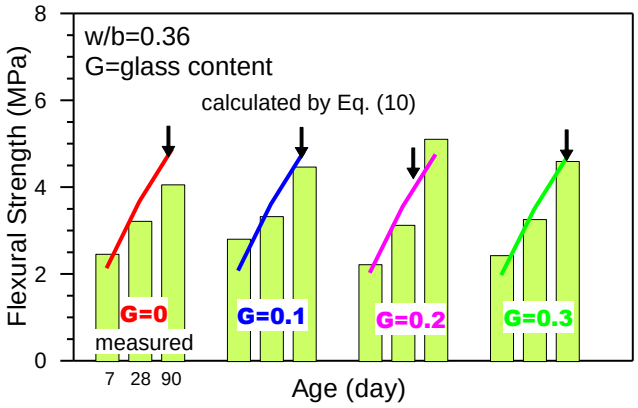

Fig. 13 Comparison results of predicted model and test results for flexural strength at w/b=0.36

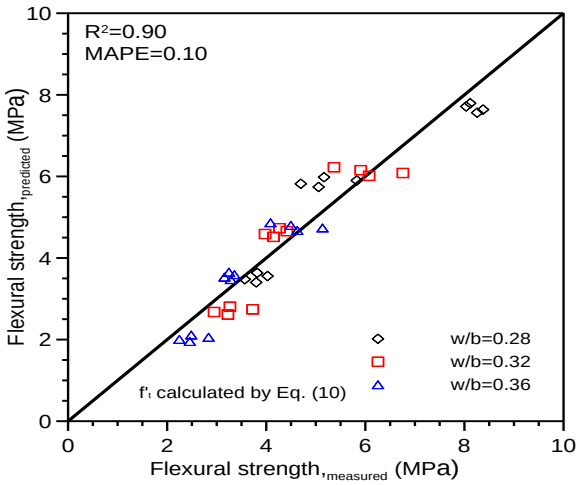

Fig. 14 Comparison of predicted and measured flexural strength

5.3 Ultrasonic pulse velocity

As shown in Fig. 15, the ultrasonic-pulse-velocity prediction model (Eq. (16)) is applied to analyze the ultrasonic pulse velocity and the testing results for concretes with different waste glass contents when the water-binder ratio is 0.28. As shown in Fig. 15, the ultrasonic-pulse-velocity prediction model based on the power function can accurately evaluate the relationships between the age and the ultrasonic pulse velocity at different waste glass contents G. The comparison between the predicted ultrasonic pulse velocities using the model and the actual experimental values was shown in Table 5.

In addition, the coefficient of determination R^2 was obtained from the regression analysis using the model for the predicted ultrasonic pulse velocity analysis value and the test result: when w/b is 0.28, $R^2 = 0.88$; when w/b is 0.32, $R^2 = 0.87$; when w/b is 0.36, $R^2 = 0.89$. The analytic result shows that the MAPE value is 1.8%, 2.1% and 2.2% when the water-binder ratio w/b is 0.28, 0.32 and

0.36, respectively. The comparison of all water-binder ratio analysis values and testing results suggest that the coefficient of determination is R^2 = 0.90, which is greater than 0.8, and MAPE = 2.1%, as shown in Fig. 16 and Table 6. Therefore, the ultrasonic-pulse-velocity prediction model also has excellent prediction abilities.

Fig. 17 illustrates the relationship between the compressive strength and the ultrasonic pulse velocity for concretes with different waste glass contents when the water-binder ratio is 0.28. As shown in Fig. 17, the prediction analysis results of the compressive strength and the ultrasonic pulse velocity using Eqs. (6) and (16) are notably similar to the testing results, and they have a notably good linear relationship. Similarly, other water-binder ratio testing results have an identical tendency as suggested by Wang (2009) in the study of waste LCD glass concrete. Moreover, when the prediction analysis accuracy of the compressive strength and ultrasonic pulse velocity is

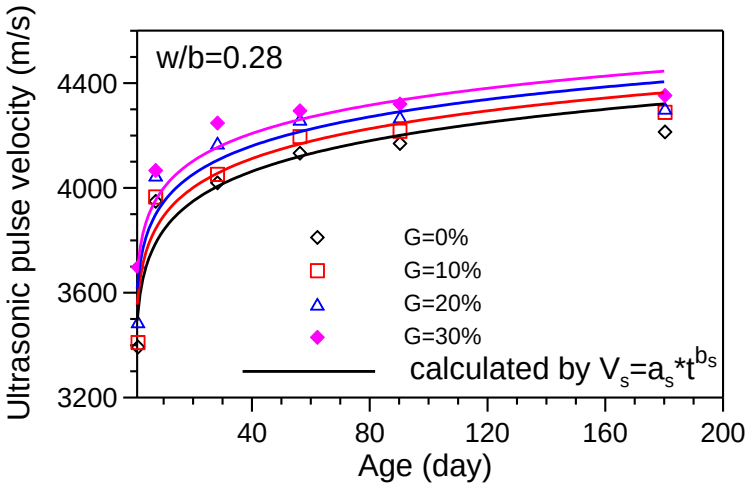

Fig. 15 Comparison results of predicted model and test results for Ultrasonic pulse velocity

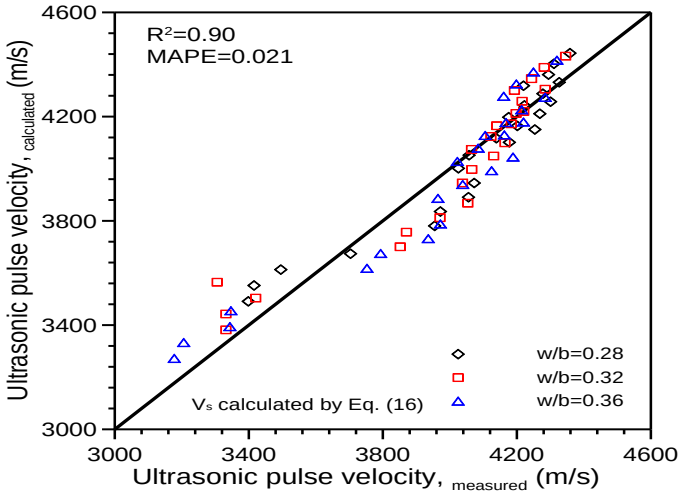

Fig. 16 Comparison of predicted and measured ultrasonic pulse velocity

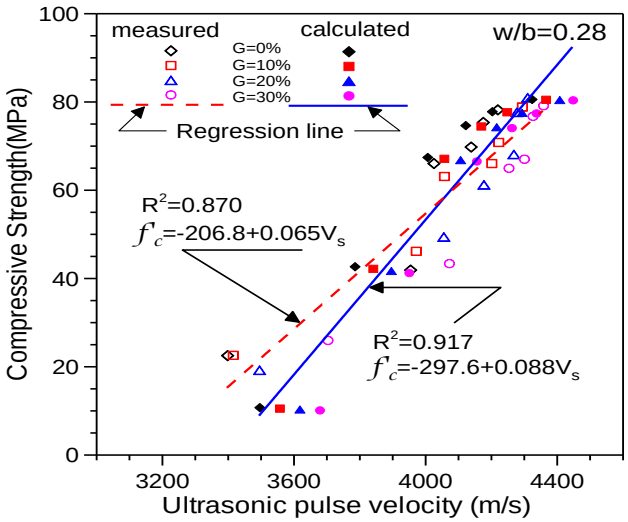

Fig. 17 Relationship of compressive strength and ultrasonic pulse velocity

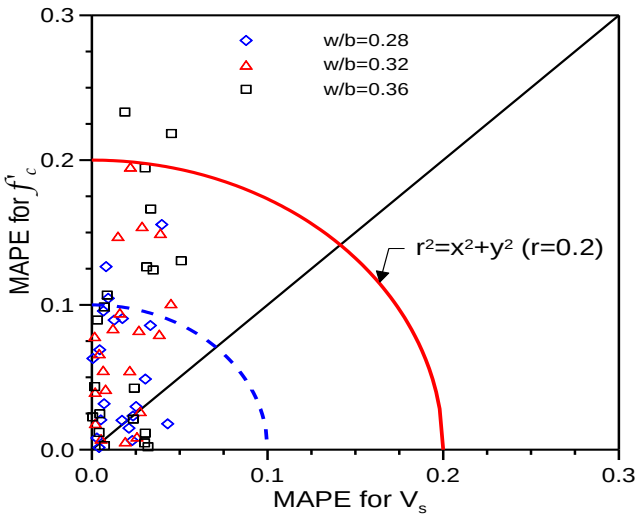

Fig. 18 Comparison of MAPE values for compressive strength and ultrasonic pulse velocity

compared, most MAPE values are in the range of 0.2; in particular, the ultrasonic-pulse-velocity MAPE value is below 5% as shown in Fig. 18. Therefore, the proposed compressive-strength and ultrasonic-pulse-velocity analysis models have good prediction capabilities.

6. Conclusions

1. By coupling a hyperbolic function, an exponential function and a power function with waste glass concrete hardened properties, we developed a prediction analysis model that considers the compressive strength, flexural strength and ultrasonic pulse velocity of the concrete with

multiple variables such as the water-binder ratio, waste glass content and age. The findings of this study can serve as a reference for the future design of mixing ratios of waste LCD glass concrete.

2. Compared with the testing result, the statistical analysis shows that the coefficient of determination R^2 and the MAPE (mean absolute percentage error) were obtained in the range of 0.93–0.96 and 5.4–8.4% for the compressive strength, 0.83–0.89 and 8.9–12.2% for the flexural strength, and 0.87– 0.89 and 1.8–2.2% for the ultrasonic pulse velocity, respectively. R^2=0.83 is obviously slightly lower than 0.85, and MAPE=12.2% is slightly higher than 10% for only the flexural-strength analysis. However, the values of R^2 and MAPE are more than 0.87 and less than 10% compared with the other analyses, respectively. Therefore, the predicted models of compressive strength, flexural strength and ultrasonic pulse velocity that are proposed in this paper exhibit good predictive capabilities.

3. The compressive strength f'_c and flexural strength f'_t of a specimen increased with age but decreased when the water-binder ratio increased. For the same mixture ratio, the compressive strength of specimen f'_c decreased when the waste glass content increased, which is consistent with previous studies. However, the flexural strength f'_t is not significantly affected by the waste glass content. The ultrasonic pulse velocity tends to increase with increasing waste glass content. The applicability of the prediction model of various hardening mechanical properties, which was established using deduction and the tendency of the testing results, to other mixing conditions remains to be studied and verified in the future.

References

Ahmed, S.F.U. (2013), "Properties of concrete containing construction and demolition wastes and fly ash", *J. Mater. Civ. Eng., ASCE*, **25**(12), 1864-1870.

Al-Shamrani, M.A. (2005), "Applying the hyperbolic method and Ca/Cc concept for settlement prediction of complex organic-rich soil formations", *Eng. Geology*, **77**, 17-34.

Atis, C.D., Karahan, O., Ari, K., Sola, O.C. and Bilim, C. (2009), "Relation between Strength Properties (Flexuraland Compressive) and Abrasion Resistance of Fiber (Steel and Polypropylene)-Reinforced Fly Ash Concrete", *J. Mater. Civ. Eng., ASCE*, **21**(8), 402-408.

Barbuta, M., Diaconescu, R.M and Harja, M. (2012), "Using Neural Networks for Prediction of Properties of Polymer Concrete with Fly Ash", *J. Mater. Civ. Eng., ASCE*, **24**(5), 523-528.

Boscardin, M.C., Selig, E.T., Lin, R.S. and Yang, G.R. (1990), "Hyperbolic parameters for compacted soils", *Journal of Geotechnical Engineering, ASCE*, **116** (1), 88-104.

Cheng, A., Hsu, H.M., Chao, S.J. and Lin, K.L. (2011), "Experimental Study on Properties of Pervious Concrete Made with Recycled Aggregate", *Int. J. Pav. Res. Technol.* , **4**(2), 104-110.

Ciou, S.S. (2009), "A study on the high temperature properties of cement mortar with waste liquid crystal glass powder", Master Dissertation, National Kaohsiung University of Applied Sciences, Kaohsiung.

Dapena, E., Alaejos, P., Lobet, A. and Pérez, D. (2011), "Effect of Recycled Sand Content on Characteristics of Mortars and Concretes", *J. Mater. Civ. Eng., ASCE*, **23**(4), 414-422.

Duncan, J.M. and Chang, C.Y. (1970), "Nonlinear analysis of stress and strain in soil", *J. Soil Mech. Found. Div., ASCE*, **96**(SM5), 1629-1653.

Gao, Y.Y., Liu, L.P. and Wang, Y.J. (2008), "LCD panel manufacturing waste resource status of Comment. Green Foundation newsletters", special reports.

Huang, W.L. (2009), "A study on waste LCD glass applied in self-compacting concrete", Master Dissertation, National Kaohsiung University of Applied Sciences, Kaohsiung.

Hwang, K., Noguchi, T. and Tomosawa, F. (1999), "Numerical prediction model for compressive strength

development of concrete containing fly ash", *J. Struct. Constr. Eng., Architect. Inst. Japan*, **519**, 1-6.
Ismail, Z.Z. and Hashmi, E.A.A. (2009), "Recycling of waste glass as a partial replacement for fine aggregate in concrete", *Waste Manage.*, **29**, 655-659.
Konder, R.L. (1963), "Hyperbolic stress–strain response: cohesive soils", *J. Soil Mech. Found. Div., ASCE*, **89** (1), 115-143.
Kou, S.C. and Poon, C.S. (2009), "Properties of self-compacting concrete prepared with recycled glass aggregate", *Cement Concrete Compos*, **31**, 107-113.
Kumar, B., Tike, G.K. and Nanda, P.K. (2007), "Evaluation of Properties of High-Volume Fly-Ash Concrete for Pavements", *J. Mater. Civ. Eng., ASCE*, **19**(10), 906-911.
Lewis, C.D. (1982), *Industrial and Business Forecasting Method.*, London: Butterworth Scientific Publishers, London.
Lin, K.L. (2007), "The effect of heating temperature of thin film transistor-liquid crystal display (TFT-LCD) electric-optical waste glass substitute partial clay as eco-brick", *J. Cleaner Product.*, **15**, 1755-1759.
Lin, K.L., Huang, W.J., Shie, J.L., Lee, T.C., Wang, K.S. and Lee, C.H. (2009), "The utilization of thin film transistor liquid crystal display waste glass as a pozzolanic material", *J. Hazard. Mater*, **163**, 916-921.
Lin, K.L., Shiu, H.S., Shie, J.L., Cheng, T.W. and Hwang, C.L. (2012), "Effect of composition on characteristics of thin film transistor liquid crystal display (TFT-LCD) waste glass-metakaolin -based geopolymers", *Constr. Build. Mater.*, **36**, 501-507.
Mousavi, S.M., Aminian, P., Gandomi, A.H., Alavi, A.H. and Bolandi, H. (2012), "New predictive model for compressive strength of HPC using gene expression programming", *Adv. Eng. Softw.*, **45**, 105-114.
Murat, P., Erdogan, O., Ahmet, O. and Ishak Yuce, M. (2007), "Appraisal of long-term effects of fly ash and silica fume on compressive strength of concrete by neural networks", *Constr. Build. Mater.*, **21**, 384-394.
Park, S.B., Lee, B.C. and Kim, J.H. (2004), "Studies on mechanical properties of concrete containing waste glass aggregate", *Cement Concrete Res.*, **34**, 2181-2189.
Shah, A.A., Alsayed, S.H., Abbas, H. and Al-Salloum, Y.A. (2012), "Predicting residual strength of non-linear ultrasonically evaluated damaged concrete using artificial neural network", *Constr. Build. Mater.*, **29**, 42-50.
Sridharan, A. and Rao, S.N. (1972), "Hyperbolic representation of strength, pore pressures and volume changes with axial strain in triaxial tests", *Proceedings of the Symposium on Strength and Deformation Behaviour of Soils*, Bangalore, India, 33-42.
Stark, T.D., Ebling, R.M. and Vettel, J.J. (1994), "Hyperbolic stress–strain parameters for silts", *J. Geotech.Eng., ASCE*, **120** (2), 420-441.
Tang, C.W. (2014), "Producing synthetic lightweight aggregates by treating waste TFT-LCD glass powder and reservoir sediments", *Comput. Concr.*, **13**(2), 149-171.
Terro, M.J. (2006), "Properties of concrete made with recycled crushed glass at elevated temperatures", *Build. Environ.*, **41**, 633-639.
Topcu, I.B. and Canbaz, M. (2004), "Properties of concrete containing waste glass", *Cement Concrete Res.*, **34**, 267-274.
Vahid, K.A. and Mohammad, T. (2010), "Prediction of 28-day compressive strength of concrete on the third day using artificial neural networks", *Int. J. Eng.*, **3**(6), 565-576.
Wang, C.C. (2001), "Time-dependent hyperbolic model for clayey soil", *J. Chinese Inst. Civil Hydraulic Engineering* ,Chinese, August.
Wang, C.C., Chen, T.T., Wang, H.Y. and Huang, C. (2014), "A predictive model for compressive strength of waste LCD glass concrete by nonlinear-multivariate regression", *Comput. Concr.*, **13**(4), 531-545.
Wang, H.Y. (2009), "A study of the engineering properties of waste LCD glass applied to controlled low strength materials concrete", *Constr. Build. Mater.*, **23**, 2127-2131.
Wang, H.Y. (2011), "The effect of the proportion of thin film transistor–liquid crystal display (TFT–LCD) optical waste glass as a partial substitute for cement in cement mortar", *Constr. Build. Mater.*, **25**, 791-797.
Wang, H.Y. and Chen, J.S. (2008), "Study of thin film transition liquid crystal display(TFT-LCD) optical waste glass applied in early-high-strength controlled low strength materials", *Comput. Concr.*, **5**, 491-501.

Wang, H.Y. and Huang, W.L. (2010a), "A study on the properties of fresh self-consolidating glass concrete (SCGC)", *Constr. Build. Mater.*, **24**, 619-624.
Wang, H.Y. and Huang, W.L. (2010b), "Durability of self-consolidating concrete is using waste LCD glass", *Constr. Build. Mater.*, **24**, 1008-1013.
Wang, H.Y., Chen, J.S., Wang, S.Y., Chen, Z.C. and Chen, F.L. (2007), "A study on the mix proportion and properties of wasted LCD glass applied to controlled low strength materials concrete (CLSM)", *J. Taiwan Concrete Institute*.

CC